Two-Dimensional Effects on the in Situ Infrared Spectra of CO Adsorbed at Palladium-Covered Pt(111) Electrode Surfaces

B. Álvarez, A. Rodes,* J. M. Pérez, and J. M. Feliu

Departamento de Química Física, Universidad de Alicante, Apartado 99, E-03080 Alicante, Spain

Received: July 31, 2002; In Final Form: December 20, 2002

The in situ infrared spectra obtained for CO-saturated palladium layers deposited on Pt(111) and several vicinal surfaces are analyzed in this paper by correlating the observed C−O stretching bands with the cyclic voltammogram recorded for the corresponding surface before CO dosing. In the case of the Pt(111) electrode, results are reported in the whole palladium coverage range from (sub)monolayers to multilayers. For palladium coverages up to the monolayer, the C−O stretching spectra are consistent with previous results suggesting the formation of wide epitaxial islands upon palladium deposition. Increasing the palladium coverage above the monolayer on the Pt(111) electrode gives rise to a splitting of the C−O stretching band in the region between 1900 and 1950 cm^{-1}. This splitting is also observed when a palladium monolayer is deposited on surfaces vicinal to the Pt(111) surface irrespective of the (111) or (100) orientation of the step sites in the corresponding regular terrace−step structure. Decreasing the terrace width favors the high-frequency feature, which could be related to CO adsorbed on terrace sites near the step edge. When comparing this effect of the size of the two-dimensional palladium domains on the frequency of the C−O stretching band with the spectra obtained for the palladium-covered Pt(111) surface, it can be suggested that palladium films does not grow layer-by-layer once the first layer is completed.

1. Introduction

Fundamental aspects of reactivity in electrochemical systems can be approached through the controlled modification of well-defined single crystal electrode surfaces. The resulting adlayers have electrochemical properties that may be different both from those of the underlying substrate and from those of the bulk deposited material. As a typical example involving noble metals, palladium films can be deposited on platinum[1−9] and gold[10−12] electrodes with coverages ranging from (sub)monolayers to multilayers. Different papers have been published in past years regarding both the preparation and the characterization of these bimetallic surfaces. Palladium deposition methods included electrochemical deposition,[3,8−12] vapor vacuum deposition,[5,6,13] and the so-called forced deposition method.[2,4,7,14,15] On the other hand, palladium films have been characterized both ex situ, with standard ultrahigh vacuum (UHV) techniques,[5,6,13] and in situ, by using scanning tunneling microscopy (STM),[11,12] SXS,[8] infrared spectroscopy,[3,7,9,13−16] and cyclic voltammetry.[2,4,9,14,15] In this latter case, the voltammetric characterization of the palladium-covered electrodes relies on the existence of coupled reversible hydrogen/anion adsorption/desorption processes that give rise to characteristic and structure-sensitive voltammetric features that can be related to the amount of deposited palladium.[4,9] Voltammetric criteria exist also to distinguish the deposition of palladium in a first layer from deposition in the second and subsequent layers.[4,9] As a related point, it can be recalled here that the charge displacement technique has been employed to determine the potential of zero total charge (pztc) for palladium-covered Pt(111) electrodes as a function of the amount of deposited palladium.[9,17] It was found that the changes of the pztc in sulfuric acid solutions with the palladium coverage follows different trends before and after the completion of the first layer that correlated well with the infrared spectra of adsorbed (bi)sulfate anions.[9,17]

Additional information on the palladium films deposited on platinum electrodes has been obtained by using probe molecules such as carbon monoxide[3,13−16] and nitric oxide.[7] Inukai and Ito[3] obtained the infrared spectra for CO adsorbed at Pt(100) and Pt(111) single crystal electrodes covered with (sub)-monolayers of palladium deposited electrochemically. More recently, Arenz et al.[13] reported similar C−O stretching spectra for palladium-covered Pt(111) electrodes in alkaline solutions. The surface structure of palladium multilayers deposited on Pt-(110),[14] Pt(100),[15] and Pt(111)[18] have also been characterized with adsorbed CO. The good agreement between the spectra for the CO-saturated palladium-covered surfaces and those reported for Pd(*hkl*) surface in a vacuum[19−21] suggested that the palladium films grow epitaxially on the platinum substrate.

In the case of palladium monolayers, conclusions derived from the infrared spectra[16] are in good agreement with data derived from in situ surface X-ray scattering experiments.[8] The latter indicated that palladium is deposited on the Pt(111) substrate as a uniform epitaxial metallic layer having the same lattice constant as that of the platinum substrate.[8] However, the existence of two-dimensional order in the surface structure of palladium layers above the monolayer is still open to discussion. This point, which cannot be resolved from the voltammetric data alone, is related to the growing mode of the palladium layer and can be addressed by analyzing the C−O stretching spectra of palladium surfaces with different degrees of surface order. This could be done either by employing palladium stepped surfaces or by depositing palladium monolayers on platinum stepped substrates with different orientations. This latter approach will be used in this paper, where the spectra for CO adsorbed on Pt(111) electrodes previously covered with palladium at coverages above the monolayer will be reported. Then,

* Corresponding author. E-mail: Antonio.Rodes@ua.es.

10.1021/jp0266547 CCC: $25.00
Published on Web 02/08/2003

these spectra will be compared with those corresponding to palladium monolayers formed on platinum electrodes with orientations vicinal to Pt(111) in the [1$\bar{1}$0] and [0$\bar{1}$1] zones. These electrodes have orientations that correspond to regular terrace−step surface structures with (111) terraces separated by (111) or (100) steps, respectively.[22,23] Changing the surface orientation with respect to the (111) pole allows the width of the (111) terraces to be varied in a controlled way. In this way, the role of the two-dimensional long-range order of the electrodeposited palladium film on the corresponding C−O stretching spectra can be investigated. The obtained spectra will be also useful for understanding the origin of some differences observed between the spectra reported for CO adsorbed on Pd-(111) electrodes[24,25] and those reported under UHV conditions.[19,20]

2. Experimental Section

Pt(111) single crystal electrode surfaces were prepared by using the method developed by Clavilier.[26] Samples employed in the infrared experiments were ca. 4.5 mm in diameter. Sulfuric and perchloric acid solutions were prepared from the concentrated acid (Merck Suprapur) and ultrapure water from a Millipore Milli-Q system. All the experiments reported in this paper were performed at room temperature. Potentials were measured against a reversible hydrogen electrode (RHE). Prior to each experiment the solution was deaerated by bubbling Ar (N50). The electrochemical deposition of palladium was carried out in a preparation cell, containing a diluted Pd^{2+} (10^{-5} M) solution in 0.1 M sulfuric acid. The clean, flame-annealed, Pt-(111) electrode was cycled between 1.0 and 0.06 V in the palladium-containing solution at a sweep rate of 50 mV s^{-1}, and the corresponding voltammograms were recorded. Once the desired palladium coverage was attained, the electrode was rinsed with water and transferred to a spectroelectrochemical cell[27] containing a 0.1 M perchloric acid solution. This cell was provided with a prismatic CaF_2 window beveled at 60°.

Fourier transform infrared spectroscopic (FTIR) experiments were performed with a Nicolet Magna 850 spectrometer equipped with an MCT detector. Single beam spectra were collected at a given potential with p-polarized light and a resolution of 8 cm^{-1}. The spectra for the CO-covered electrode are represented as the ratio $-\log(R/R_0)$, where R and R_0 are the reflectance values corresponding to the sample and reference single beam spectra, respectively. The reference spectrum was taken at 1.0 V after the oxidative stripping of adsorbed CO. Typically, 100 interferograms were coadded to obtain each single beam spectrum.

3. Results

3.1. Voltammetric Characterization of the Palladium-Covered Pt(111) Electrodes. Figure 1 shows typical cyclic voltammograms obtained in the 10^{-5} M Pd^{2+} + 0.1 M H_2SO_4 solution for a Pt(111) electrode covered with layers of palladium atoms at different coverage values. Cyclic voltammograms in Figure 1A correspond to the very first stages of palladium deposition. Except for the couple of sharp peaks at 0.23 V, these curves are similar to the characteristic voltammogram recorded for the clean and well-ordered Pt(111) electrode in the 0.1 M H_2SO_4 solution.[2,4,9] These peaks are related to the coupled adsorption/desorption of hydrogen and (bi)sulfate anions at the palladium atoms deposited in a first layer[2,4,9] and can be used to monitor the electrodeposition process in the (sub)monolayer range. In this respect, the palladium coverage in this coverage range can be estimated from the charge density under the peak at 0.23 V.[4,9]

Note that the voltammetric currents between 0.33 and 0.80 V corresponding to the adsorption/desorption of (bi)sulfate anions on the platinum atoms decrease steadily in Figure 1A as the peaks at 0.23 V are developed with cycling. These contributions are hardly observed in the cyclic voltammogram in Figure 1B, which is characteristic of a palladium coverage value close to the monolayer. An additional pair of small peaks at 0.28 V in this curve is associated with the same processes taking place on palladium atoms deposited over the first layer.[4,9,17] As described in detail elsewhere, these peaks appear before the complete blockage of the platinum substrate for a palladium coverage value of ca. 0.95.[9] The voltammogram in Figure 1B corresponds to a compromise between the maximum blockage of the platinum substrate and a minimum extent of the deposition of palladium atoms in a second layer. A similar voltammetric profile was reported by Markovic et al. for an epitaxial monolayer of palladium atoms deposited on a Pt(111) electrode surface.[8]

The deposition of additional amounts of palladium with respect to the experiments reported in Figure 1A,B can be easily achieved by increasing the deposition time (i.e., the numbers of potential cycles). In this way, the voltammetric curve in Figure 1C has been obtained for a surface for which a significant portion of the first layer of palladium has been covered by additional palladium atoms. This process gives rise to an increase of the peak at 0.28 V, which is paralleled by the decrease of the peak at 0.23 V in the voltammogram. From the charge density obtained upon integration of the peak at 0.23 V in Figure 1C, it can be estimated that half of the first layer of palladium remains available for adsorption from solution. Finally, the absence of a well-developed peak at 0.23 V in the voltammogram in Figure 1D indicates that nearly all the palladium atoms in the first layer of the corresponding surface are covered by at least one additional palladium atom. The existence of several palladium layers over the platinum substrate is also suggested by the increase in the voltammetric current below 0.10 V, which can be ascribed to hydrogen absorption at the palladium-covered electrode.

3.2. Spectroscopic Characterization of the Palladium-Covered Pt(111) Electrodes. Palladium-covered Pt(111) electrodes can be further characterized by analyzing the spectra obtained upon saturation with adsorbed CO. The spectra reported in the following were obtained in the spectroelectrochemical cell, containing a 0.1 M $HClO_4$ solution, where the palladium-covered electrodes were transferred from the deposition cell once the desired palladium coverage was attained. After dosing CO at 0.10 V for 2 min, the solution was purged by bubbling Ar (5 min) and a series of single beam spectra was collected at various electrode potentials up to 1.0 V. The cyclic voltammogram obtained for the resulting surface between 0.05 and 0.40 V (not shown here) indicates a complete blockage of the palladium surface atoms by adsorbed CO. In addition, it has been verified that the voltammetric curves obtained after the oxidation of the CO adlayer fit in all cases with that recorded for the same sample before the adsorption of CO. This proves that the CO adsorption and oxidation processes do not induce significant changes in the palladium adlayer, irrespective of the palladium coverage.

Figure 2 shows two sets of spectra obtained, respectively, at 0.10 and 0.50 V for the saturated CO adlayer formed on the bare (bottom spectra) and palladium-covered Pt(111) electrodes with palladium coverages increasing up to the monolayer (top spectra). The spectra reported in Figure 2 for the CO-saturated Pt(111) electrode are similar to those previously published by different research groups.[28−31] The spectrum collected at 0.10

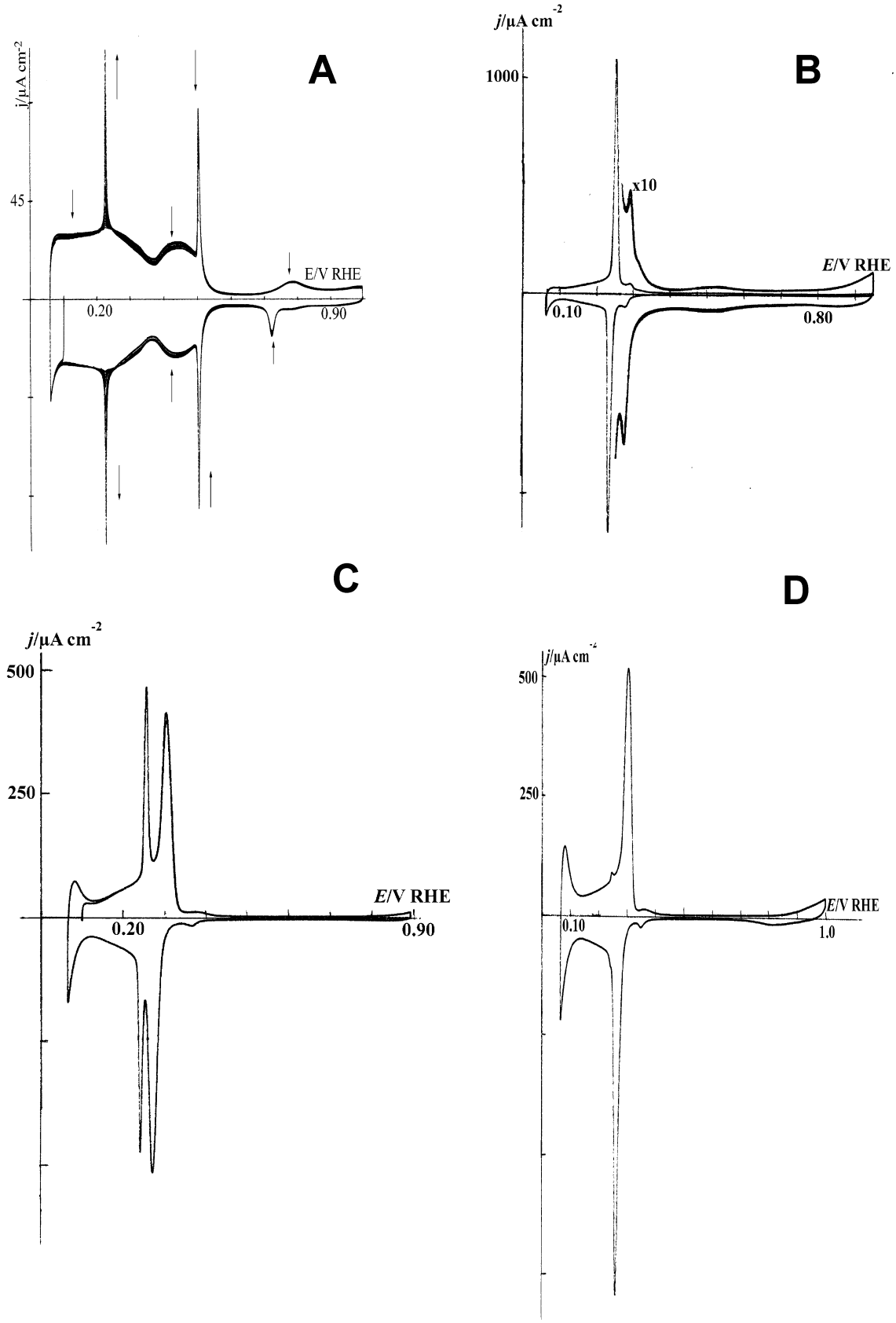

Figure 1. Cyclic voltammograms for a Pt(111) electrode in a 10^{-5} M Pd^{2+} + 0.1 M H_2SO_4 solution at different stages of palladium deposition. See text for details. Sweep rate: 50 mV s^{-1} (the same for all voltammetric experiments).

V is characterized by absorption bands at 2065 and 1779 cm^{-1}, which can be assigned to the C−O stretching vibrations of atop and 3-fold hollow CO molecules, respectively. This spectrum can be considered as a fingerprint for the existence of surface domains covered by a (2 × 2)-3CO adlayer.[29,30] Increasing the electrode potential up to 0.50 V gives rise to the blue shift of the band initially at 2065 cm^{-1}. At the same time, the intensity of the lower frequency feature decreases as it is replaced by an

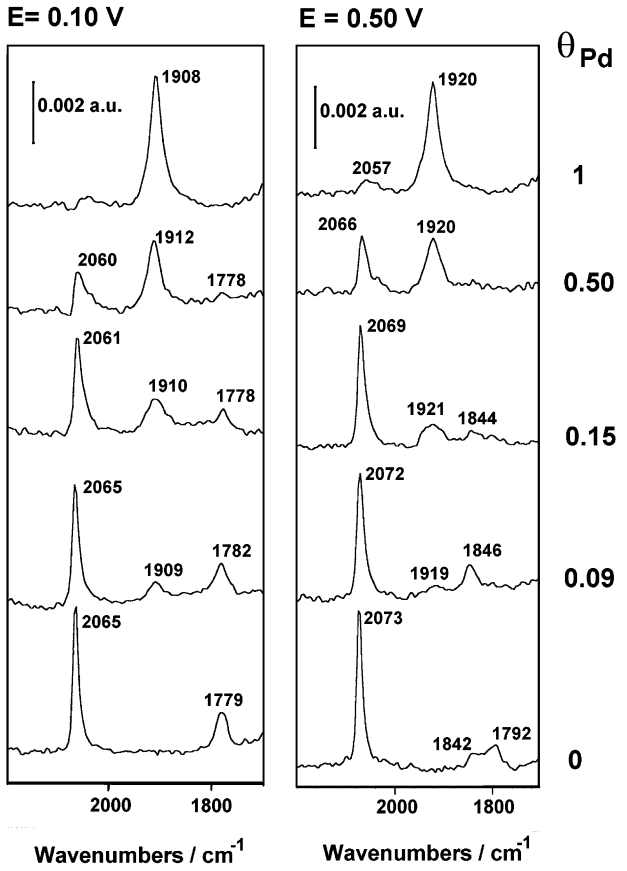

Figure 2. In situ infrared spectra for CO-saturated palladium-covered Pt(111) electrodes in the (sub)monolayer range. One hundred interferograms were collected for each single beam spectrum at 8 cm^{-1} (same conditions for all the infrared experiments).

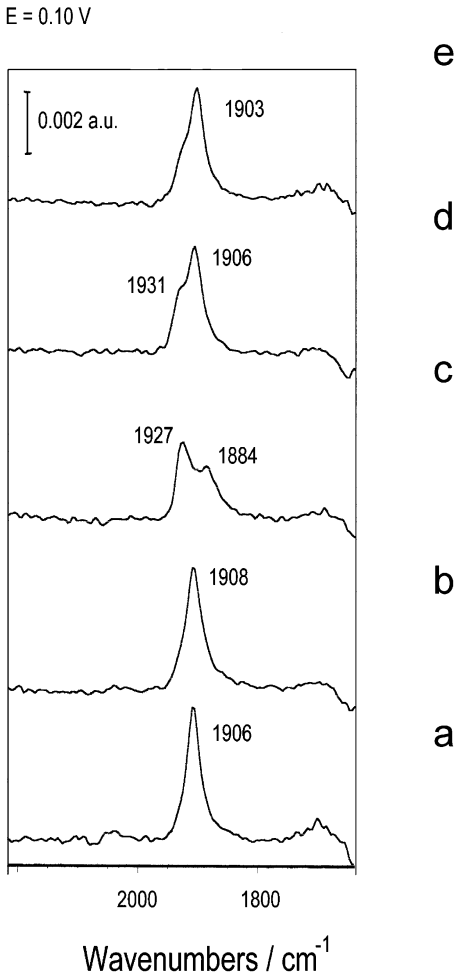

Figure 3. In situ infrared spectra for CO-saturated palladium-covered Pt(111) electrodes in the multilayer range (see text for details).

absorption band at 1847 cm^{-1}, which has been assigned to the C−O stretching vibration of bridge bonded CO molecules. This latter change has been interpreted as a result of the disappearance of the ordered (2 × 2)-3CO structure.[29,30] The exact electrode potential at which this transformation takes place depends mainly on the actual CO coverage,[30,32] the long-range bidimensional order at Pt(111) substrate,[30] and the existence of coadsorbed anions.[33] When CO is present in the working solution, the (2 × 2)-3CO structure can be retained at potentials as high as 0.60 V for well-ordered Pt(111) electrodes.[30,32] This situation corresponds to the existence of a uniform (2 × 2)-3CO adlayer with the highest CO coverage of 0.75. In the absence of dissolved CO, the slightly lower CO coverages obtained from the stripping experiments suggest the coexistence of patches with the (2 × 2)-3CO structure and regions with a less dense CO adlayer.[30]

The top spectra reported in Figure 2 were collected for the saturated CO adlayer formed on the palladium-covered electrode giving rise to the cyclic voltammogram reported in Figure 1B. The spectrum at 0.10 V shows a main C−O stretching band at 1908 cm^{-1} which is shifted upward when the electrode potential is polarized at 0.50 V. The spectra collected at this electrode potential show a small band around 2050 cm^{-1}. This latter feature may correspond to CO adsorbed on small uncovered platinum areas since it disappears when additional amounts of palladium are deposited (see the spectra in Figure 3). Note that no other band appears in the spectral region around 1900 cm^{-1} irrespective of the electrode potential.

Figure 2 also shows spectra for partially covered surfaces, i.e., with palladium coverages which are intermediate between those corresponding to the voltammetric curves in Figure 1A,B. All these spectra show distinct features characteristic of CO adsorbed on platinum and CO adsorbed on palladium atoms. In this respect, the spectra collected at 0.10 V for the partially covered surfaces show always the band at ca. 1780 cm^{-1} previously described for the palladium-free Pt(111) surface. Increasing the electrode potential up to 0.50 V gives rise to the typical transformation of this band into a band at ca. 1845 cm^{-1}. Since these features are highly sensitive to the existence of long-range order in the platinum domains, it can be concluded that the palladium layer is growing uniformly in such a way that uncovered domains with long-range order still exist at the electrode surface at intermediate palladium coverages. At the same time, the band for CO adsorbed on palladium in Figure 2 is observed at a given potential at nearly the same frequency, irrespective of the palladium coverage. This behavior can be observed in Figure 4, where the C−O stretching frequency for platinum (curves a−c) and palladium (curve d) domains are plotted as a function of the electrode potential for the spectra reported in Figure 2. The constancy of the C−O stretching frequency in these spectra also suggests the formation of relatively wide palladium islands where the coupling effects between the adjacent CO molecules does not depend anymore on the island size. On the other hand, it has to be noted that the band for atop CO on the platinum atoms is slightly red-shifted, broadens, and becomes asymmetric (with a tail at the lower wavenumbers) as the palladium coverage increases. This behavior can be related to a decrease in the dimension of the platinum domains as palladium coverage approaches unity. The

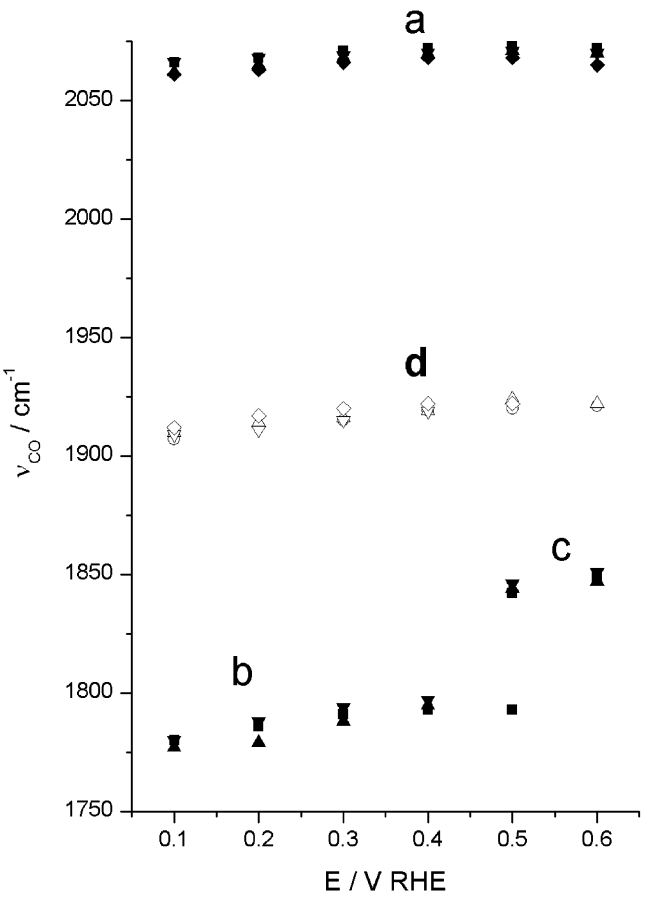

Figure 4. Plot of the C−O stretching frequency for the bands observed in the experiments reported in Figure 2 as a function of the electrode potential. Full symbols correspond to atop (curve a), 3-fold hollow (curve b), and bridge (curve c) bands for CO adsorbed on platinum sites whereas open symbols correspond to bridge bands for CO adsorbed on palladium sites (curve d). Palladium coverage varies as follows: 0 (■); 0.09 (▽, ▼); 0.15 (△, ▲); 0.50 (◇, ◆); 1 (○).

spectra reported in Figure 2 for partially covered surfaces and the conclusions derived from the effect of palladium coverage on the intensity and frequency of the observed C−O stretching bands are similar to those reported by Arentz et al. in alkaline solutions.[13] These spectra are also similar to those previously reported by Ito et al.[3] for a Pt(111) electrode immersed in a 10^{-4} M $PdCl_2$ solution except for the observation, under these experimental conditions and irrespective of the palladium coverage, of two well-marked palladium contributions in the C−O stretching region between 1900 and 1950 cm^{-1}. This difference can be related to the presence of a relatively high concentration of palladium ions in the working solution that could give rise to changes in the palladium coverage during the collection of the infrared spectra. As will be discussed bellow, the observation in the spectra reported by Ito's group of more than one absorption band for CO adsorbed on palladium atoms can be related to the onset of the deposition of a second layer of palladium atoms before the completion of the first layer.

Figure 3 reports a series of spectra collected at 0.10 V for CO-saturated Pd/Pt(111) electrodes with coverages above the monolayer (spectra b−e). The spectrum for the palladium monolayer (spectrum a) is shown again in this figure for the sake of comparison. Spectra c and e in Figure 3 correspond to voltammograms C and D, respectively, in Figure 1. On the other hand, spectra b and d were collected for surfaces with palladium coverages between those corresponding to Figure 1B and 1C (spectrum b) and between those for Figure 1C and 1D (spectrum

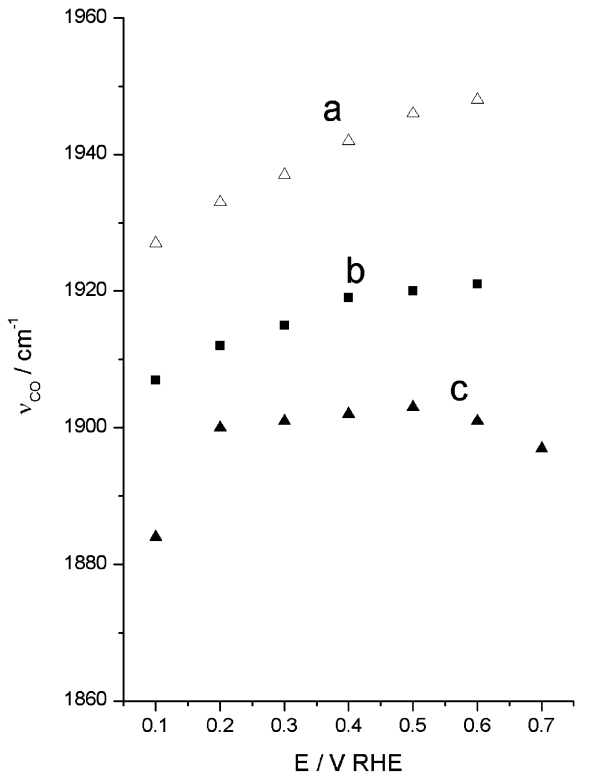

Figure 5. Plot of the potential-dependent C−O stretching frequency for the bands observed in the experiments reported in Figure 3, spectra a (curve a) and c (curves b and c).

d). Changes in the spectra reported in Figure 3 concern the broadening and subsequent splitting of the observed C−O stretching band. These changes can be analyzed in connection with the relative intensity of the voltammetric peaks at 0.23 and 0.28 V in Figure 1. In this way, the development of the peak at 0.28 V when the palladium coverage is increased above the monolayer parallels the broadening (spectrum b) and then the splitting of the C−O stretching band (spectrum c). Two C−O stretching bands at 1927 and 1884 cm^{-1} in the spectra collected at 0.10 V for the surface give rise to a cyclic voltammogram in the sulfuric acid solution with nearly equal peaks at 0.23 and 0.28 V (spectrum c). As the amount of deposited palladium is further increased, the intensity of the band at 1927 cm^{-1} in spectrum c decreases and becomes a shoulder in spectrum e. The main C−O stretching band in this spectrum appears at 1906 cm^{-1}.

The most striking result in Figure 3 is the splitting of the C−O stretching band in spectrum c. As advanced in ref 16, this splitting is maintained in the whole potential range up to the onset of CO oxidation. Curves b and c in Figure 5 show plots of the C−O stretching wavenumber as a function of the electrode potential for the bands in spectrum c in Figure 3. From this plot it can be clearly observed that the frequency of the high-frequency feature (curve b) in this spectrum is significantly blue-shifted in comparison with the C−O stretching band for the palladium monolayer (curve a), whereas the low-frequency band appears at lower wavenumbers. In addition, curves a and b in Figure 5 show linear variations of the C−O stretching frequency with the electrode potential up to 0.50 V with tuning rates of ca. 33 and 47 cm^{-1} V^{-1}, respectively.

3.3. Spectroscopic Characterization of Palladium-Covered Platinum Stepped Electrodes. Figure 6 shows series of voltammograms obtained for a Pt(17,15,15) stepped surface in the 10^{-5} M Pd^{2+} + 0.1 M H_2SO_4 solution. This surface is vicinal to Pt(111) in the [0$\bar{1}$1] zone, and its orientation corresponds to

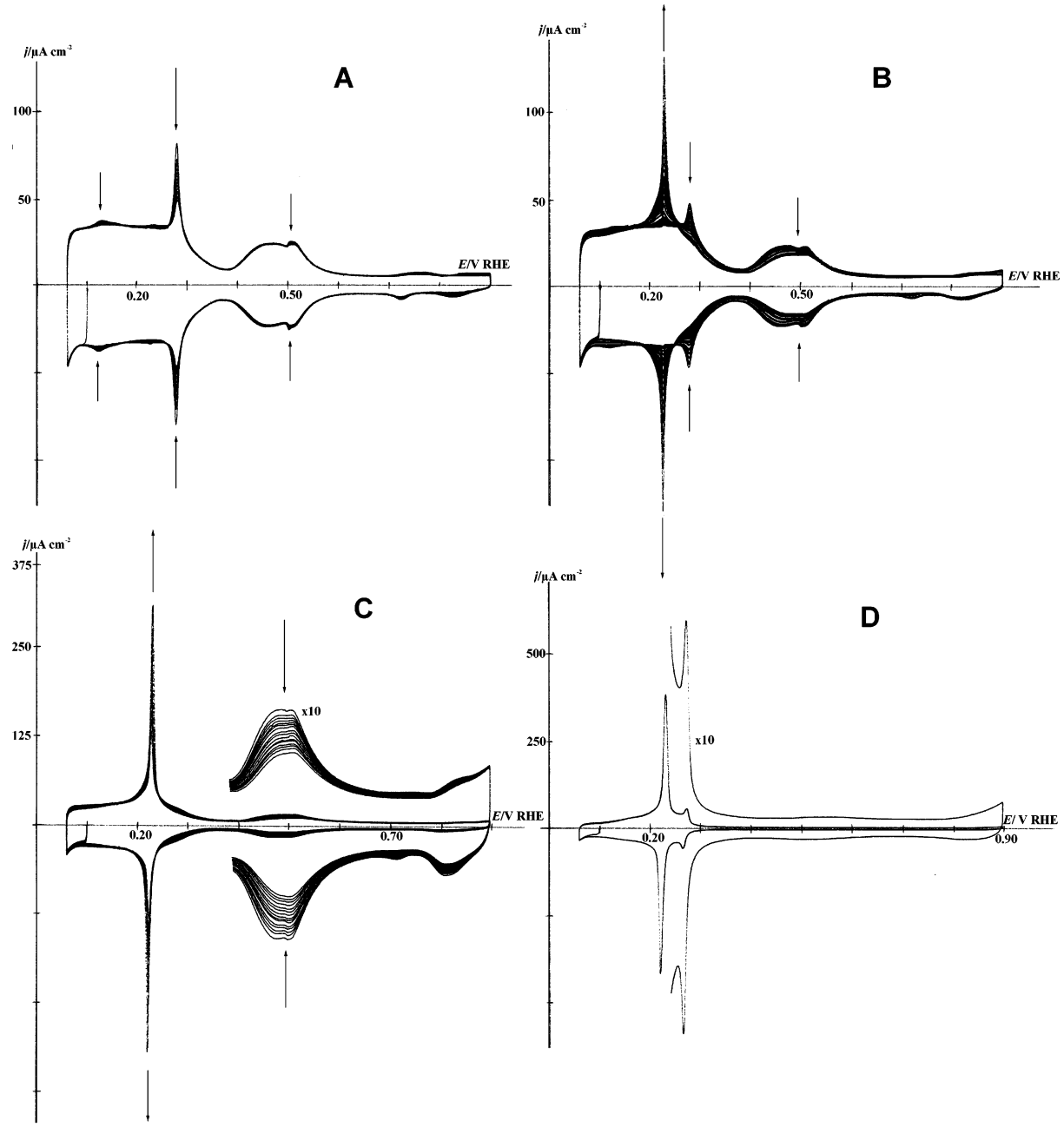

Figure 6. Cyclic voltammograms for a Pt(17,15,15) electrode in a 10^{-5} M Pd^{2+} + 0.1 M H_2SO_4 solution at different stages of palladium deposition. See text for details.

a regular Pt(S)[17(111) × (100)] surface structure with 17 atomic rows wide (111) terraces separated by monatomic (100) steps. The presence of the (100) sites in the surface structure is evidenced by the appearance of a pair of reversible voltammetric peaks at 0.28 V.[23] Cycling this surface in the palladium-containing solution causes the characteristic peaks for hydrogen and anion adsorption at platinum (111) and (100) sites to be blocked by deposited palladium atoms (Figure 6A). The faster decrease of the peak initially at 0.28 V indicates that palladium deposition proceeds at the (100) steps faster than at the (111) terraces. This also occurs with the (110) surface defects whose adsorption state initially at 0.10 V is readily blocked upon palladium deposition. Then, the characteristic peak at 0.23 V for palladium deposited at the (111) terrace appears with further cycling (Figure 6B) and adsorption states at potentials above 0.35 V for anion adsorption at platinum (111) terraces become blocked (Figure 6B,C). The voltammogram in Figure 6D, which is similar to that in Figure 1B for Pt(111), corresponds to a surface state with the palladium coverage around the monolayer. As in the case of the Pt(111) electrode, the nearly flat current region above 0.3 V indicates that most of the platinum sites are covered by a first layer of palladium atoms whereas the small peak at 0.28 V indicates that deposition of the second layer has started in a small fraction of the surface. The observation of a lower peak current for the palladium peak at 0.23 V in Figure 6D can be related to the existence of narrower (111) terraces in the Pt(17,15,15) substrate when compared to Pt(111).

The trends observed during palladium deposition on Pt(17,-15,15) are similar to those observed for other stepped surfaces vicinal to Pt(111) with different terrace width and/or step symmetry. As additional examples, Figure 7 reports the cyclic voltammograms for the palladium monolayers formed at Pt-(17,15,15) and Pt(322) surfaces, which correspond to regular Pt(S)[17(111) × (111)] and Pt(S)[5(111) × (100)] surface structures, respectively. As expected from the existence similar

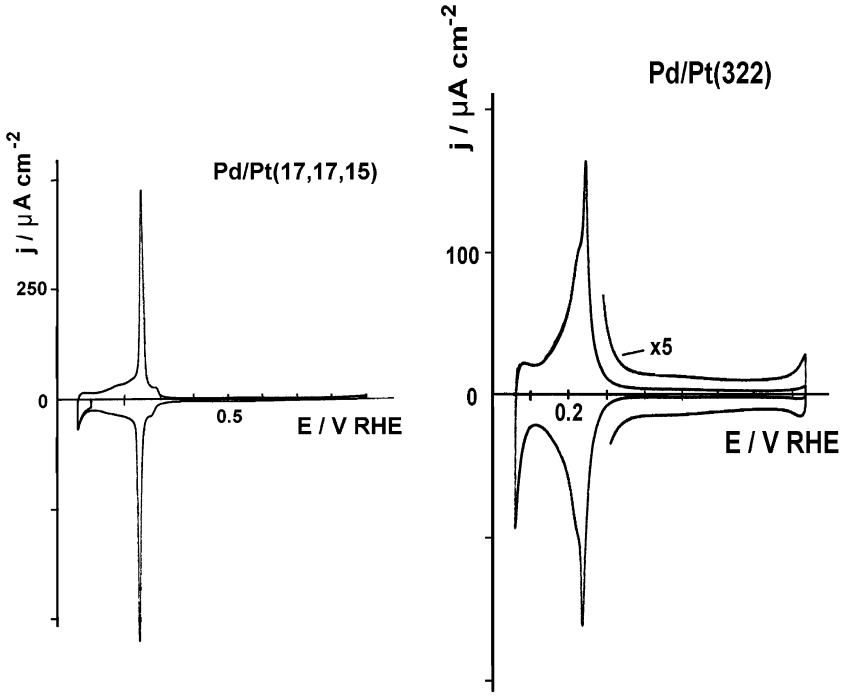

Figure 7. Cyclic voltammograms for a monolayer of palladium deposited on Pt(17,17,15) and Pt(322) electrodes.

terrace widths, the curves for the palladium-covered Pt(17,15,-15) and Pt(17,17,15) electrodes in Figures 6D and 7 are quite similar. Regarding the voltammogram for the palladium-covered Pt(322) electrode, Figure 7 shows the existence of a broad and less intense peak at 0.23 V which fits with the existence of narrow (111) terraces. We can conclude from Figures 6 and 7 that the peak potentials at 0.23 and 0.28 V are characteristic of palladium deposition at platinum (111) terraces in a first and second layer of atoms, respectively, irrespective of the terrace width at least down to five atomic rows. On the other hand, it seems reasonable to conclude from the maximum development of the peak at 0.23 V and the nearly complete blockage of adsorption states above 0.30 V for platinum that a palladium monolayer has been deposited in all cases. Such monolayers could be expected to be similar to the corresponding Pd(*hkl*) surfaces in terms of terrace and step orientations, terrace width, and step height.

Spectroscopic experiments with the palladium-covered stepped surfaces were performed with Pt(17,17,15) and Pt(443) electrodes in the $[1\bar{1}0]$ zone (the latter surface corresponding to a Pt(S)[8(111) × (111)] surface structure) and with Pt(17,17,15) and Pt(322) electrodes in the $[0\bar{1}1]$ zone. The potential-dependent spectra reported in Figures 8 and 9 correspond to the CO-saturated surface in each case, always with a palladium coverage around the monolayer. Figure 10 allows the comparison between the spectra collected at 0.10 V for the CO-saturated palladium monolayers deposited on these stepped surfaces and that collected for the palladium monolayer deposited on Pt(111). Spectra for the palladium-covered Pt(17,17,15) and Pt(17,15,15) surfaces in Figure 10 show a clear-cut splitting of the C−O stretching band with absorption maxima at ca. 1928 and 1906 cm^{-1}. For surfaces with narrower terraces, the higher frequency band is shifted upward. Conversely, the intensity of the low-frequency band, which can be observed as a shoulder in the spectra for the Pd/Pt(433) surface, is significantly decreased. An additional band at ca. 2035 cm^{-1} in the spectra of Pd/Pt(322) and Pd/Pt(433) surfaces could be ascribed in a first approximation to atop CO adsorbed on uncovered platinum atoms. However, this assignment would disagree with the voltammetric behavior of the palladium-covered samples, which indicates the absence of a significant amount of uncovered platinum sites. An alternative explanation would involve the ascription of the observed band to atop CO adsorbed at palladium atoms, particularly those defining step sites. This interpretation is consistent with the observation in Figure 10 of

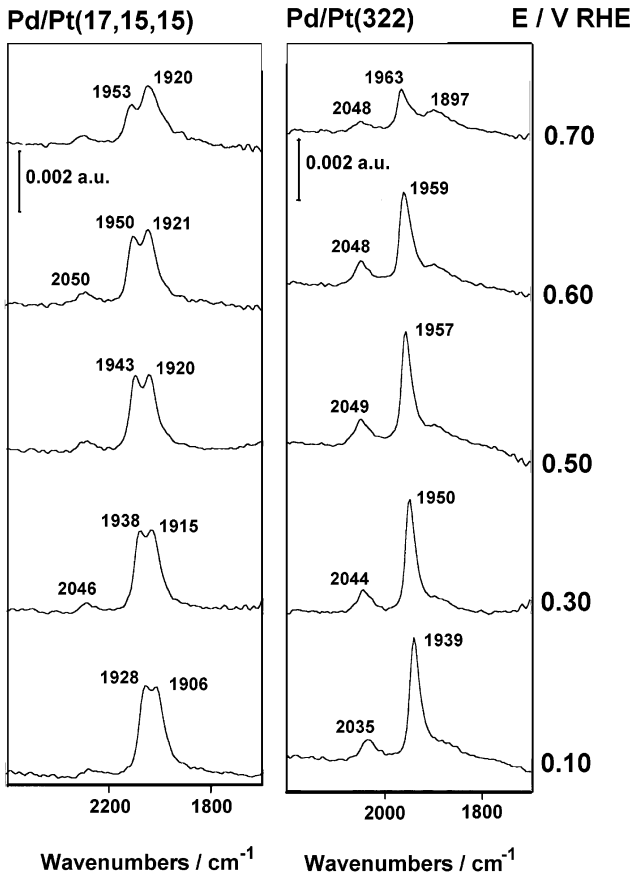

Figure 8. In situ potential-dependent infrared spectra for CO adsorbed at saturation on a palladium monolayer deposited on Pt(17,15,15) and Pt(322) electrodes.

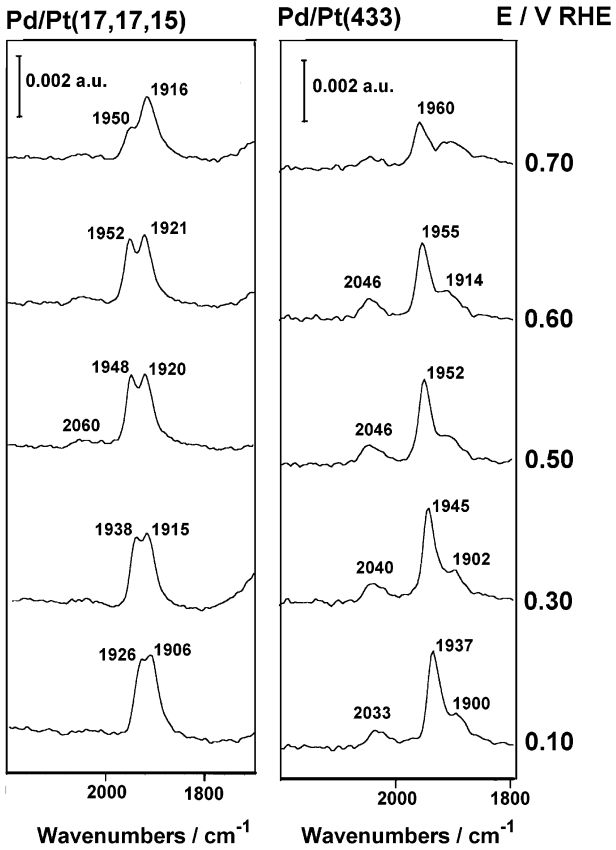

Figure 9. In situ potential-dependent infrared spectra for CO adsorbed at saturation on a palladium monolayer deposited on Pt(17,17,15) and Pt(433) electrodes.

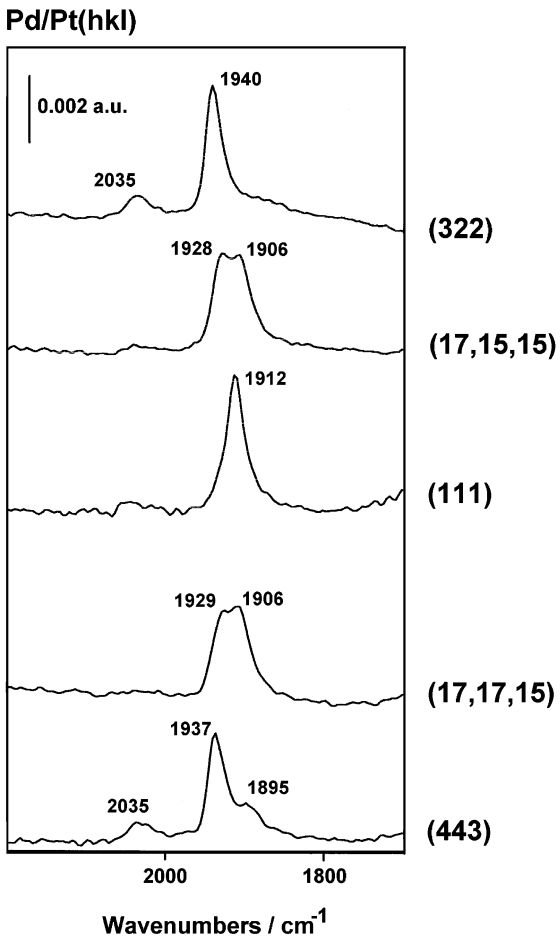

Figure 10. In situ infrared spectra at 0.10 V for CO adsorbed at saturation on a palladium monolayer deposited on Pt(111) and on vicinal surfaces in the [0$\bar{1}$1] and [1$\bar{1}$0] zones.

more intense bands at 2035 cm^{-1} for the palladium films formed at the platinum surfaces with a higher density of steps, i.e., for the Pd/Pt(433) and for the Pd/Pt(322) electrodes. In addition, this interpretation would agree with the observation of bands in the same frequency range in the case of evaporated palladium films, supported palladium particles, and unsupported palladium particles.[20,34]

From the spectra shown in Figures 8 and 9 it can be appreciated that the splitting in the C−O stretching spectra for the Pd/Pt(17,15,15) and Pd/Pt(17,17,15) surfaces is more clearly appreciated at high electrode potentials, just below the onset of the CO electrooxidation process. This latter reaction starts at ca. 0.70 V as evidenced by the decrease in the intensity of the CO bands and the observation of the characteristic band at 2344 cm^{-1} for dissolved CO_2 (not shown). It has to be also noted that the intensity of the high-frequency band decreases first when the oxidation of the CO adlayer starts. Regarding the effect of the electrode potential on the C−O stretching frequency, it has to be remarked that both bands are shifted upward as the electrode potential increases but with a higher tuning rate for the high-frequency feature. This point can be clearly appreciated in Figure 11, where the C−O stretching frequencies for the different Pd/Pt(*hkl*) stepped surfaces studied are compared with those for the Pd/Pt(111) surface. Whereas the plots for the low-frequency band for Pd/Pt(17,15,15) and Pd/Pt(17,17,15) fit with that of Pd/Pt(111), with a tuning rate of ca. 35 cm^{-1} V^{-1}, the tuning rates for the corresponding high-frequency feature are 51 and 55 cm^{-1} (measured in all cases for potentials up to 0.50 V). These values are similar to that corresponding to the plot in Figure 5, curve b, for the Pd/Pt(111) surface when the first palladium layer is partially covered by additional palladium atoms. It can also be observed in Figure 11 how the C−O stretching frequency for the high-frequency feature increases at constant potential as the width of the underlying platinum terraces decreases for Pd/Pt(443) ($n = 8$) and Pd/Pt(322) ($n = 5$). The observed tuning rates measured for these surfaces are 38 and 44 cm^{-1} V^{-1}, respectively.

4. Discussion and Conclusions

The spectra discussed above for the palladium-covered electrodes can be compared with those previously reported for CO adsorbed on palladium surfaces under UHV conditions. First, it has to be stated that the spectrum described under these conditions for the Pd(111) surface at half coverage[19,20] is similar to that reported for the CO-saturated palladium monolayer in Figure 2, which corresponds to a CO coverage of around 0.55.[9] The lower frequency for the band observed under electrochemical conditions is a well-known consequence of the existence of a lower surface potential.[35] The ascription of the observed C−O stretching frequency to a given adsorption site is not straightforward and can be different depending on the structure of the CO adlayer. In this way, photoelectron diffraction studies at 200 K showed that a mixture of fcc and hcp hollow sites are occupied by adsorbed CO in the $c(4 \times 2)$-2CO structure,[36] for which a single band in the infrared spectra was located at 1920 cm^{-1}.[19,20] Calculated frequencies by Loffreda et al.[37] for the corresponding $c(4 \times 2)$-2CO structure with hcp and fcc occupied hollow sites agree quite well with this result. The adsorption of CO on hollow sites at low temperature (120 K) is also supported by recent high-resolution XPS experiments reported by Surnev

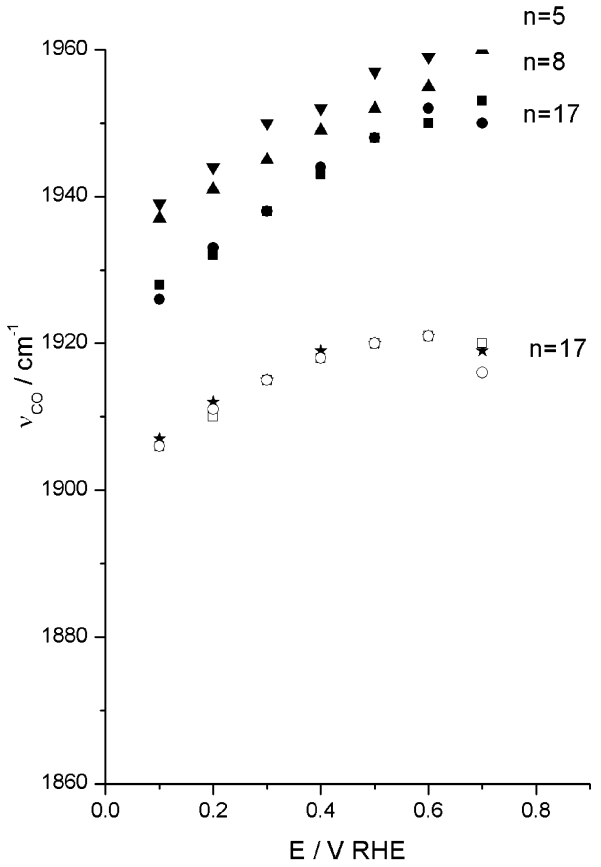

Figure 11. Plot of the potential-dependent C−O stretching frequency for the bands observed in the spectra reported in Figures 8 and 9. Legend: (■, □) Pt(17,15,15); (●, ○) Pt (17,17,15); (△, ▲) Pt(433); (▽, ▼) Pt (322); (★) Pd/Pt(111) (monolayer).

et al.[38] However, the results obtained by the same authors at 300 K suggest a different picture, with bridge adsorption being dominant at 0.5 monolayer coverage with domain boundary regions which introduce poor long-range ordering. Here, it is worth recalling that the present electrochemical experiments are carried out at room temperature. Therefore, comparison to the experiments at 300 K noted above seems more appropriate. In a previous paper,[16] the origin of the C−O stretching band for the palladium monolayer was discussed in connection with the existing data. It was concluded in this paper that the band observed in the spectra is probably related to bridge bonded CO molecules in a disordered CO adlayer.[16] More recently, Lucas et al.[39] concluded from their SXS experiments for the CO-saturated adlayer formed on an epitaxial monolayer of palladium that either the CO layer is disordered or it forms an incommensurate structure. Thus, the broadness of the band at 1908 cm^{-1}, when compared to that of the band at 2065 cm^{-1} for Pt(111), which can also be influenced by the ordering of the underlying palladium layer, seems to be mainly related to the ordering of the CO adlayer.

The next point to be considered is that of the origin of the differences between the spectrum discussed above for the palladium monolayers and those reported in Figures 3 and 8−10. These differences concern the splitting of the absorption band around 1900 cm^{-1} and, in some cases, the observation of an additional band in the atop C−O stretching region. It has to be noted first that spectrum c in Figure 3 is similar to those previously reported by Yoshioka et al. for a flame-annealed Pd(111) electrode[24] and by Zou et al. for an electropolished Pd(111) electrode.[25] For these surfaces, a pair of bands was observed at 1940−1960 and 1890−1920 cm^{-1} depending on the CO coverage and electrode potential. Zou et al. assigned these bands to "bridging-like" along with hollow CO binding.[25] Since the band at 1940−1960 cm^{-1} has no counterpart for Pd(111) under UHV conditions, it was proposed that it could be related to water coadsorption.[25] However, spectra reported in Figure 3 suggest another explanation for the splitting of the C−O stretching band, which is related to the growing mechanism of palladium films once the palladium monolayer is completed. Whereas a layer-by-layer (or Frank−van der Merwe) growth mode has been suggested by Attard's group for evaporated palladium under UHV conditions,[5] in situ X-ray diffraction experiments carried out by Markovic et al.[40] for electrodeposited palladium films on Pt(111) indicates a different growing mechanism. These authors found that, even if the palladium deposit keeps on growing in registry with the substrate, the second layer of palladium atoms was not completed before the deposition of third and next layers started, giving rise to an increase of the surface roughness. Thus, surfaces associated with voltammetric curves such as that in Figure 1C seem not to be strictly flat. In other words, the two-dimensional order of the outmost palladium layer would be lower than that for the surface corresponding to Figure 1B (full monolayer). The changes observed in the corresponding C−O stretching spectra strongly suggest that the C−O stretching frequency on palladium is highly sensitive to the size of the palladium domains. In this way, the disappearance of the splitting in the spectrum corresponding to the voltammogram in Figure 1D could be related to the observation by Markovic et al. of quite a flat surface when palladium multilayers (ca. 10 layers thick) are deposited.[40] Finally, it could be concluded from this discussion that the Pd(111) surfaces resulting from the flame annealing or the electropolishing treatments are less ordered than those obtained under UHV conditions or by slow electrodeposition of a palladium monolayer on a well-ordered Pt(111) electrode.

The hypothesis assumed in the preceding paragraph could be checked easily by studying the effect of varying the dimension of the bidimensional domains in a controlled way. Since palladium stepped surfaces are not available in our laboratory, our strategy involved the deposition of palladium monolayers on stepped platinum electrodes. We assume that the palladium films created under these conditions match the surface structure of the underlying platinum substrate. The spectra reported in Figures 8−10 show that the splitting of C−O stretching band in the region between 1900 and 1950 cm^{-1} is also observed when a palladium monolayer is deposited on surfaces vicinal to the Pt(111) surface irrespective of the (111) or (100) orientation of the step sites in the corresponding regular terrace−step structure. Decreasing the terrace width favors the high-frequency feature, which could be related to CO adsorbed on bridge sites near the step edges in a first approximation.

Another characteristic feature in the spectra for the stepped Pd/Pt(*hkl*) surfaces is the band at 2035−2050 cm^{-1}, whose intensity also increases as the terrace width of the underlying platinum substrate decreases. Here again these observations can be compared with data, obtained either in situ or under UHV conditions, for systems for which the role of the two-dimensional order of the palladium domains on the corresponding adsorption properties have been analyzed. In this respect, it is worth mentioning here recent results published by Maroun et al.[41] on the adsorption properties of electrodeposited PdAu alloys on Au(111) single crystal electrodes. These authors used STM images to determine the distribution of palladium and gold atoms as a function of the alloy composition. Then, the role of atomic ensembles toward CO adsorption was derived from the corre-

sponding in situ infrared spectra. The band for atop CO was observed in the spectra for alloys with a very low surface concentration of palladium for which palladium monomers predominate. Conversely, absorption bands in the bridge region are only observed for surfaces with a palladium surface content higher than 22%. STM images for these surfaces showed the presence of palladium dimers and trimers. Increasing the palladium surface content above 22% gives rise to a decrease of the intensity of the atop C−O stretching band and a parallel increase of the band in the bridge region, which becomes predominant for a pure palladium film. Although the authors do not discuss this point in detail, it has to be noted that the bridge CO contribution observed in the C−O stretching spectra appears first as a broad adsorption band that sharpens as the palladium content increases. This behavior seems to be also related to the existence of wider palladium domains. A similar explanation could be given to the observation reported by Nishimura et al.[42] of a bridge band at higher frequencies in the PM-IRRAS spectra of CO adsorbed at the surface of bulk PdAu alloys when compared to that observed for a pure Pd electrode surface.

To our knowledge, there are a limited number of papers describing the spectra for CO adsorbed on stepped palladium surfaces under UHV conditions.[19,20,43] Bradshaw and Hoffmann reported the C−O stretching spectra for the Pd(210) surface,[19,20] whereas Svensson et al. described the HREELS spectra for CO adsorbed on the Pd(510) surface.[43] Both stepped surfaces contain narrow (100) terraces (two and five atoms rows wide, respectively) separated by (110) steps. The spectra obtained for the Pd(210) surface are similar to those reported for the Pd(100), suggesting that CO molecules are adsorbed in bridge sites in both cases.[19,20] On the other hand, the spectra reported for the Pd(510) surface shows an atop CO contribution that is not observed for the Pd(100) surface and can be ascribed to CO adsorbed on step sites.[43] However, this contribution appears at the highest CO coverages and corresponds to binding energy lower than that for CO adsorbed on the terrace sites. This behavior contrasts with results obtained for a Pd(211)═Pt(S)-[3(111) × (100)] surface for which CO adsorbs preferentially at the step sites.[44]

Another set of relevant UHV data concerns the behavior of palladium crystallites deposited on different substrates.[45] As typical examples, Wolter et al.[46,47] and Giorgi et al.[48] studied the structure and adsorption properties of palladium particles deposited on alumina and on crystalline silica, respectively. These authors used adsorbed CO as a probe molecule for the characterization of these particles and correlated the infrared spectra in the C−O stretching region with the corresponding structural data derived from STM and SPA-LEED experiments. In this way, palladium particles deposited on alumina were shown to grow as crystallites with predominant (111) facets[45] whereas those grown on silica are somewhat more disordered.[48] In addition to the substrate, other factors such as the temperature of palladium deposition were shown to play a role in the size and order of the resulting particles.[45−47] When comparing the infrared spectra obtained for the CO-covered palladium particles and those obtained for Pd single crystal surfaces (especially with the Pd(111) surface), the authors reported several characteristic differences that can be related to the results presented in this paper. First of all, they observed the presence of a C−O stretching band in the region of linear bonded CO, i.e., around 2100 cm^{-1} for the CO-saturated samples under UHV conditions. The intensity of this feature, which is observed for a well-ordered Pd(111) surface only for the compressed structures formed at high CO pressures,[19,20] is higher for the smallest and less ordered particles. On the other hand, the authors reported the existence of two distinct bands in the bridge CO region, i.e., between 1900 and 2000 cm^{-1}. The band at the highest frequency in this region, between 1950 and 2000 cm^{-1}, which is dominant in the spectra and whose intensity increases with respect to that of the atop band when the size of the crystallite increases, was related to CO molecules adsorbed on edge sites. On the other hand, the frequency of the other band in the bridge CO region, between 1900 and 1950 cm^{-1}, is similar to that observed for well-ordered Pd(111) surfaces and was ascribed to CO adsorbed on the (111) facets. Even if intensity transfer phenomena favor the high-frequency feature, the spectra reported by Wolter et al. for alumina-supported particles showed that the intensity of the band at ca. 1950 cm^{-1} increases as the particle size does.[45−47]

All the results discussed above for the UHV experiments support our analysis for the C−O stretching spectra for the palladium-covered Pt(*hkl*) electrodes. In summary, we can conclude that the band at 2035 cm^{-1} is probably related for these samples to atop CO adsorbed on step sites. On the other hand, bands at ca. 1910 and 1940 cm^{-1} would correspond to bridge bonded CO adsorbed on (111) edge and terrace sites, respectively. On the basis of this assignment, it can be concluded that wide (111) palladium domains predominate for palladium monolayers electrodeposited on Pt(111) electrodes. At higher palladium coverages, the splitting in the C−O bridge region of the infrared spectra suggests that two-dimensional long-range order decreases probably related to the deposition of palladium atoms at third and subsequent layers before the second layer is completed. This behavior is related to the observation of two voltammetric hydrogen/anion adsorption/desorption peaks, namely at 0.23 and 0.28 V, for the C−O free surfaces in sulfuric acid solution. When the latter peak predominates, i.e., when palladium multilayers are electrodeposited, the C−O stretching spectrum is similar to that of the palladium monolayer, thus suggesting that the outmost palladium layer is relatively flat. The existence of such a flat electrode surface makes the corresponding palladium films a good alternative to bulk palladium single crystal electrodes.

Acknowledgment. This work has been financed by the Ministerio de Ciencia y Tecnología (Spain) in the framework of Project BQU2000-0240. B.Á. is grateful for the award of a Ph.D. grant from the Ministerio de Educación y Cultura (Spain). Funds provided by the Conselleria de Cultura, Educació i Ciència de la Generalitat Valenciana for the purchase of the FTIR facility are also acknowledged.

References and Notes

(1) Attard, G. A.; Bannister, A. *J. Electroanal. Chem.* **1991**, *300*, 467.
(2) Clavilier, J.; Llorca, M. J.; Feliu, J. M.; Aldaz, A. *J. Electroanal. Chem.* **1991**, *310*, 429.
(3) Inukai, J.; Ito, M. *J. Electroanal. Chem.* **1993**, *358*, 307.
(4) Llorca, M. J.; Feliu, J. M.; Aldaz, A.; Clavilier, J. *J. Electroanal. Chem.* **1993**, *351*, 299.
(5) Attard, G. A.; Price, R.; Al-Akl, A. *Electrochim. Acta* **1994**, *39*, 1525.
(6) Attard, G. A.; Price, R. *Surf. Sci.* **1995**, *335*, 63.
(7) Alvarez, B.; Rodes, A.; Perez, J. M.; Feliu, J. M.; Rodriguez, J. L.; Pastor, E. *Langmuir* **2000**, *16*, 4695.
(8) Markovic, N. M.; Lucas, C. A.; Climent, V.; Stamenkovic, V.; Ross, P. N. *Surf. Sci.* **2000**, *465*, 103.
(9) Alvarez, B.; Climent, V.; Rodes, A.; Feliu, J. M. *J. Electroanal. Chem.* **2001**, *497*, 125.
(10) Baldauf, M.; Kolb, D. M. *Electrochim. Acta* **1993**, *38*, 2145.
(11) Naohara, H.; Ye, S.; Uosaki, K. *J. Phys. Chem. B* **1998**, *102*, 4366.

(12) Naohara, H.; Ye, S.; Uosaki, K. *J. Electroanal. Chem.* **2001**, *500*, 435.
(13) Arenz, M.; Stamenkovic, V.; Schmidt, T. J.; Wandelt, K.; Ross, P. N.; Markovic, N. M. *Surf. Sci.* **2002**, *506*, 287.
(14) Gómez, R.; Rodes, A.; Pérez, J. M.; Feliu, J. M.; Aldaz, A. *Surf. Sci.* **1995**, *327*, 202.
(15) Gomez, R.; Rodes, A.; Perez, J. M.; Feliu, J. M.; Aldaz, A. *Surf. Sci.* **1995**, *344*, 85.
(16) Gil, A.; Clotet, A.; Ricart, J. M.; Illas, F.; Alvarez, B.; Rodes, A.; Feliu, J. M. *J. Phys. Chem. B* **2001**, *105*, 7263.
(17) Feliu, J. M.; Álvarez, B.; Climent, V.; Rodes, A. In *Thin Films. Preparation, Characterization, and Applications*; Soriaga, M. P., Stickney, J., Bottomley, L. A., Kim, Y.-G., Eds.; Kluwer Academic: New York, 2002; p 37.
(18) Gómez, R. Tesi Doctoral, Universitat d'Alacant, 1994.
(19) Bradshaw, A. M.;Hoffmann, F. M. *Surf. Sci.* **1978**, *72*, 513.
(20) Hoffmann, F. M. *Surf. Sci. Rep.* **1983**, *3*, 107.
(21) Raval, R.; Harrison, M. A.; King, D. A. *Surf. Sci.* **1989**, *211*−*212*, 61.
(22) Clavilier, J.; El Achi, K.; Rodes, A. *Chem. Phys.* **1990**, *141*, 1.
(23) Rodes, A.; El Achi, K.; Zamakhchari, M. A.; Clavilier, J. *J. Electroanal. Chem.* **1990**, *284*, 245.
(24) Yoshioka, K.; Kitamura, F.; Takeda, M.; Takahashi, M.; Ito, M. *Surf. Sci.* **1990**, *227*, 90.
(25) Zou, S. Z.; Gómez, R.; Weaver, M. J. *J. Electroanal. Chem.* **1999**, *474*, 155.
(26) Clavilier, J.; Armand, D.; Sun, S.-G.; Petit, M. *J. Electroanal. Chem.* **1986**, *205*, 267.
(27) Iwasita, T.; Nart, F. C.; Vielstich, W. *Ber. Bunsen-Ges. Phys. Chem.* **1990**, *94*, 1030.
(28) Kitamura, F.; Takahashi, M.; Ito, M. *Surf. Sci.* **1989**, *223*, 493.
(29) Villegas, I.; Weaver, M. J. *J. Chem. Phys.* **1994**, *101*, 1.
(30) Rodes, A.; Gomez, R.; Feliu, J. M.; Weaver, M. J. *Langmuir* **2000**, *16*, 811.
(31) Akemann, W.; Friedrich, K. A.; Stimming, U. *J. Chem. Phys.* **2000**, *113*, 6864.
(32) Lucas, C. A.; Markovic, N. M.; Ross, P. N. *Surf. Sci.* **1999**, *425*, L381−L386.
(33) Markovic, N. M.; Lucas, C. A.; Rodes, A.; Stamenkovic, V.; Ross, P. N. *Surf. Sci.* **2002**, *499*, L149−L158.
(34) Sheppard, N.; Nguyen, T. T. *Adv. Infrared Raman Spectrosc.* **1978**, *5*, 67.
(35) Weaver, M. J.; Zou, S. Z.; Tang, C. *J. Chem. Phys.* **1999**, *111*, 368.
(36) Giessel, T.; Schaff, O.; Hirschmugl, C. J.; Fernandez, V.; Schindler, K.-M.; Theobald, A.; Bao, S.; Lindsay, R.; Berndt, W.; Bradshaw, A. M.; Baddeley, C.; Lee, A. F.; Lambert, D. K.; Woodruff, D. P. *Surf. Sci.* **1998**, *406*, 90.
(37) Loffreda, D.; Simon, D.; Sautet, P. *Surf. Sci.* **1999**, *425*, 68.
(38) Surnev, S.; Sock, M.; Ramsey, M. G.; Netzer, F. P.; Wiklund, M.; Borg, M.; Andersen, J. N. *Surf. Sci.* **2000**, *470*, 171.
(39) Lucas, C. A.; Markovic, N. M.; Ball, M.; Stamenkovic, V.; Climent, V.; Ross, P. N. *Surf. Sci.* **2001**, *479*, 241.
(40) Markovic, N. M. Personal comunication.
(41) Maroun, F.; Ozanam, F.; Magnussen, M.; Behm, R. J. *Science* **2001**, *293*, 1811.
(42) Nishimura, K.; Kunimatsu, K.; Enyo, M. *J. Electroanal. Chem.* **1989**, *260*, 167.
(43) Svensson, K.; Rickardsson, I.; Nyberg, C.; Andersson, S. *Surf. Sci.* **1996**, *366*, 140.
(44) Ramsier, R. D.; Lee, K. W.; Yates, J. T., Jr. *Surf. Sci.* **1995**, *322*, 243.
(45) Baumer, M.; Freund, H. J. *Prog. Surf. Sci.* **1999**, *61*, 127.
(46) Wolter, K.; Seiferth, O.; Libuda, J.; Kuhlenbeck, H.; Baumer, M.; Freund, H. J. *Surf. Sci.* **1998**, *402*−*404*, 428.
(47) Wolter, K.; Seiferth, O.; Kuhlenbeck, H.; Baumer, M.; Freund, H. J. *Surf. Sci.* **1998**, *399*, 190.
(48) Giorgi, J. B.; Schroeder, T.; Baumer, M.; Freund, H. J. *Surf. Sci.* **2002**, *498*, L71−L77.